REMOTE FREQUENCY CALIBRATION USING GPS CARRIER-PHASE OBSERVATION MEASUREMENT AT TL

Po-Cheng Chang, Shinn-Yan Lin, and Chia-Shu Liao
National Standard Time & Frequency Lab., TL, Taiwan
12, Lane 551, Min-Tsu Road, Sec. 5, Yang-Mei, Taoyuan, Taiwan 326
Tel: 886 3 424 5179, Fax: 886 3 424 5474, E-mail: *betrand@cht.com.tw*

Abstract

Because the GPS carrier-phase observation measurement is very precise in frequency transfer, it can be used to estimate performance of a remote frequency reference with respect to the national frequency standard. TL has already set up a prototype system for this purpose. The stability and accuracy of a DUT (device under test) at a remote site with traceability to TL's frequency standard could be obtained after data processing.

The prototype system includes the master site (herein at TL) and the remote site. At the remote site, the equipped GPS receiver runs with a DUT as its frequency reference. By performing the time difference (differences between two epochs) on carrier-phase observations, the DUT's frequency offset with respect to the GPS frequency standard can be estimated. At the master site, the GPS receiver is referenced to TL's frequency standard and the time difference and carrier-phase single difference (differences between two receivers at TL and the remote site) are performed at postprocessing. The frequency offset of the DUT relative to TL's frequency standard can be estimated in this way. Observations from the remote site could be sent to TL via the Internet.

As for the system arrangement, the IGS (International GPS Service) site TWTF at TL serves as the master site and a single-frequency GPS receiver is adopted at the remote site to cost down expenses of system set up. Data analysis is done by the lab-developed software. A common-clock short-baseline test (using TL's frequency standard) and a 270-km baseline test (using a high-performance 5071A cesium clock as the remote frequency reference) were carried out to find the system's performance. In the 270-km baseline test, a dual-frequency GPS receiver was also used at the remote site for comparison.

I. INTRODUCTION

The frequency source plays a key role in many applications, such as telecommunication networks, power systems, navigation systems, and industrial equipment systems, etc. To assure these frequency sources meet their performance requirements while in use, regular frequency calibration is important and necessary. For some 24-hour online systems, it is not easy to send their frequency sources to the national metrology institute or qualified laboratories for on-site calibration. In this situation, remote frequency calibration is a feasible solution for the customers. There are many methods to calibrate the remote

Report Documentation Page

Form Approved
OMB No. 0704-0188

1. REPORT DATE	2. REPORT TYPE	3. DATES COVERED
01 DEC 2008	**N/A**	**-**

4. TITLE AND SUBTITLE	5a. CONTRACT NUMBER
Remote Frequency Calibration Using GPS Carrier-Phase Observation Measurement At TL	5b. GRANT NUMBER
	5c. PROGRAM ELEMENT NUMBER
6. AUTHOR(S)	5d. PROJECT NUMBER
	5e. TASK NUMBER
	5f. WORK UNIT NUMBER
7. PERFORMING ORGANIZATION NAME(S) AND ADDRESS(ES) **National Standard Time & Frequency Lab., TL, Taiwan 12, Lane 551, Min-Tsu Road, Sec. 5, Yang-Mei, Taoyuan, Taiwan 326**	8. PERFORMING ORGANIZATION REPORT NUMBER
9. SPONSORING/MONITORING AGENCY NAME(S) AND ADDRESS(ES)	10. SPONSOR/MONITOR'S ACRONYM(S)
	11. SPONSOR/MONITOR'S REPORT NUMBER(S)

12. DISTRIBUTION/AVAILABILITY STATEMENT
Approved for public release, distribution unlimited

13. SUPPLEMENTARY NOTES
See also ADM002186. Annual Precise Time and Time Interval Systems and Applications Meeting (40th) Held in Reston, Virginia on 1-4 December 2008, The original document contains color images.

14. ABSTRACT

15. SUBJECT TERMS

16. SECURITY CLASSIFICATION OF:			17. LIMITATION OF ABSTRACT	18. NUMBER OF PAGES	19a. NAME OF RESPONSIBLE PERSON
a. REPORT	b. ABSTRACT	c. THIS PAGE			
unclassified	**unclassified**	**unclassified**	**UU**	**8**	

oscillators. For example, the GPSDO (GPS Disciplined Oscillator) **[1,2]** is a well-known system that has the traceability to the GPS frequency standard. In general, the GPSDO estimates time differences between the local oscillator and the GPS frequency standard using pseudo-range observations. It has good long-term stability; however, the short-term stability is not so good due to large frequency variation.

Because the time and frequency dissemination using carrier-phase observations has a higher resolution than using pseudo-range ones, TL has setup the prototype system using this technique for remote frequency calibration. In this system, the remote site could estimate frequency performance of its frequency source related to the GPS frequency standard by performing the time difference on carrier-phase observations and has the system stability about 2.0×10^{-11} per second and 2.0×10^{-13} per day. At the master site, by performing the carrier-phase single difference and time difference at postprocessing, frequency performance of the remote reference relative to TL's frequency standard can be estimated. Data of the remote site can be transferred to TL through the Internet. The combined system has a resolution higher than that of the stand-alone one because the tropospheric and ionospheric delay is effectively eliminated. Experimental results show that the system stability reaches 2.0×10^{-11} per second and 6.0×10^{-14} per day with the 270-km baseline. When in a short-baseline common-clock test, the above figures become 2.0×10^{-11} per second and 8.0×10^{-15} per day.

This paper will introduce the model of GPS carrier-phase observables and its derived formulas, then describe the calibration system arrangements, including equipments installed at the master site and the remote site, and finally compare the test results, like a common-clock short-baseline test vs. a 270-km baseline test; a single-frequency GPS receiver vs. a dual-frequency one used at the remote site, etc.

II. THE MODEL OF GPS CARRIER-PHASE OBSERVABLES

The typical model of GPS carrier-phase observables **[3,4]** is

$$\Phi_A^J = \rho_A^J + c(dt^J - dT_A) + \lambda N_A^J - d_{ion}^J + d_{trop}^J + \varepsilon_A^J \qquad (1)$$

where Φ_A^J is the carrier-phase measurement of the receiver A from the J[th] GPS satellite; ρ_A^J is the true distance between the receiver A and the J[th] GPS satellite; c is the speed of light; dt^J and dT_A represent the clock differences of the J[th] GPS satellite and the receiver A related to the GPS time respectively; λ is the GPS carrier-phase wavelength; N_A^J denotes the initial phase integer ambiguity; d_{ion}^J and d_{trop}^J are the ionospheric delay and tropospheric delay respectively; ε_A^J is the unmodeled errors primarily due to multipath, temperature variation, physical factors, etc. The units of Φ_A^J in the equation are meters. For the remote frequency calibration, the remote site's GPS receiver should be input with a DUT's reference signal to replace its internal one. Under this arrangement, the term dT_A in Equation (1) represents the time difference between the external clock and the GPS time.

In our system, the remote site performs the time difference (differences between two epochs) on carrier-phase observations to obtain the variation of dT_A, which corresponds to the frequency offset of the external clock referring to the GPS time. If the satellite signal is continuously tracked, there is no cycle slip occurring and the cycle ambiguities N_A^J remain a constant. The time difference equation from Equation (1) becomes

$$\delta\Phi_A^J = \delta\rho_A^J + c\delta dt^J - c\delta dT_A - \delta d_{ion}^J + \delta d_{trop}^J + \delta\varepsilon_A^J \qquad (2)$$

where $\delta(\cdot)$ denotes the operator for differences between two epochs. The unmodeled terms δd_{ion}^{J} and δd_{trop}^{J} can't be eliminated and are regarded as errors of the frequency offset. On the other hand, the master site has its own GPS receiver and performs the same time difference as the remote site does. Additionally, the master site performs the single difference between two receivers at postprocessing. Denote the receiver at the master site by B, and the equation of time difference & single difference becomes

$$\Delta\delta\Phi_{AB}^{J} = \Delta\delta\rho_{AB}^{J} - c\Delta\delta dT_{AB} + \Delta\delta\varepsilon_{AB}^{J} \tag{3}$$

where $\Delta(\cdot)$ represents the operator for differences between the two receivers observing the same satellite. Equation (3) assumes that the two receivers are not far from each other, so the unmodeled ionospheric and tropospheric delays between them in a local area are strongly correlated. Influences from the terms d_{ion}^{J} and d_{trop}^{J} in Equation (1) could be eliminated. Since both dT_A and dT_B refer to the same GPS time, $\Delta\delta dT_{AB}$ in Equation (3) is the variation of time difference between an external clock at the remote site and the frequency standard at the master site.

III. CALIBRATION SYSTEM ARRANGEMENTS

Figure 1 shows the block diagram of our system **[5]**. It consists of the master site and the remote site. The remote site is equipped with a DDS (Direct Digital Synthesizer) manufactured by Novatech, an Ashtech G12 single-frequency GPS receiver and an industrial PC. The IGS site TWTF at TL serves as the master site, where an Ashtech ZXII-T dual-frequency GPS receiver, a distribution amplifier, a frequency doubler, and an industrial PC are installed.

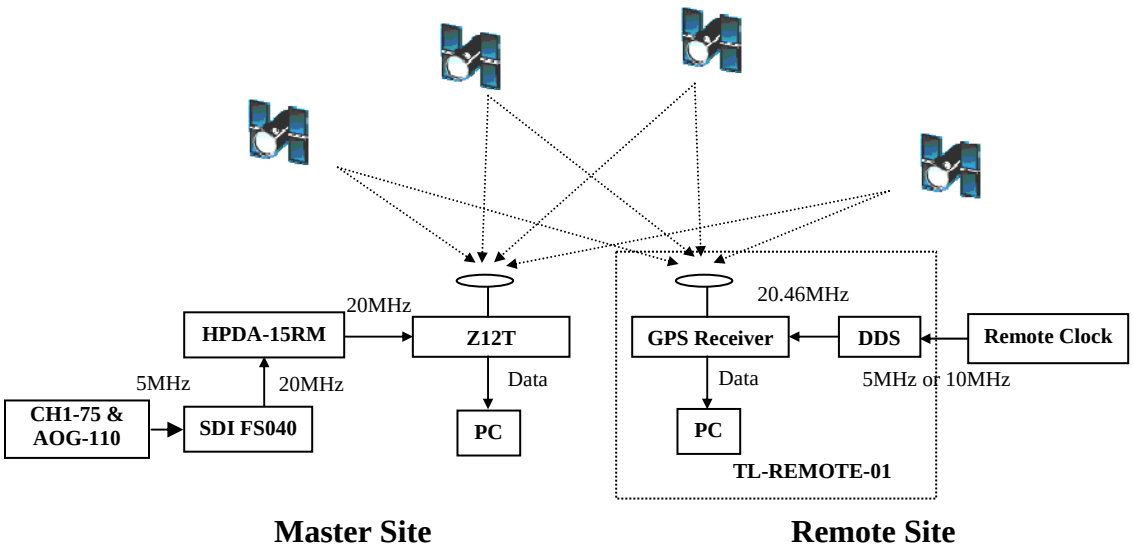

Figure 1. Block diagram of the remote frequency calibration system (RFCS) at TL.

With the help of the DDS, the frequency signal (5, 10 MHz) of a remote clock could be appropriately converted and then supplied to the GPS receiver. The single-frequency one is adopted here to cost down

equipment expenses of the remote site. By performing the time difference (i.e. (2)) on carrier-phase observations, frequency offset of the remote clock with respect to the GPS time could be estimated. Equation (2) can be further expressed as follows:

$$\delta\Phi_A^J - \delta\rho_A^J - c\delta dt^J = -c\delta dT_A - \delta d_{ion}^J + \delta d_{trop}^J + \delta\varepsilon_A^J \tag{4}$$

In Equation (4), its left-hand side is differences of the measured data and the known values. Coordinates of the remote site's GPS antenna are predetermined using the Bernese GPS software with the ones of TWTF fixed. Meanwhile, coordinates and clock errors of the GPS satellites are obtained from the broadcast navigation messages. However, the unmodeled terms δd_{ion}^J, δd_{trop}^J and some noise errors may occur in the right-hand side, which will more or less affect the estimation of related frequency offset. The term $\delta dT_A(t_i)$ **(**$= dT_A(t_i) - dT_A(t_{i-1})$, where $t_i = t_{i-1} + \tau$ **)** can be obtained by averaging (4) for all-in-view GPS observations. As previously mentioned, $\delta dT_A(t_i)$ is the time difference between the remote clock and the GPS time, the associated frequency offset $y_{gps}(t_i)$ can be expressed as

$$y_{gps}(t_i) = -\frac{\delta dT_A(t_i)}{\tau} + \frac{-\delta d_{ion}^J + \delta d_{trop}^J + \delta\varepsilon_A^J}{c\tau} = \frac{\delta\Phi_A^J - \delta\rho_A^J - c\delta dt^J}{c\tau} \tag{5}$$

At the master site, frequency offset of the remote clock with respect to the master clock can be estimated by performing the time difference and then the single difference (i.e. (3)) on carrier-phase observations. In the process, clock errors of the GPS satellites can be removed and influences of δd_{ion}^J and δd_{trop}^J significantly reduced. Equation (3) can be further expressed as follows:

$$\Delta\delta\Phi_{AB}^J - \Delta\delta\rho_{AB}^J = -c\Delta\delta dT_{AB} + \Delta\delta\varepsilon_{AB}^J \tag{6}$$

The term $\delta dT_{AB}(t_i)$ **(**$= dT_{AB}(t_i) - dT_{AB}(t_{i-1})$, where $t_i = t_{i-1} + \tau$ **)** can be obtained by averaging (6) for all in view GPS observations. Then the associated frequency offset $y_m(t_i)$ can be expressed as

$$y_m(t_i) = -\frac{\Delta\delta dT_{AB}(t_i)}{\tau} + \frac{\Delta\delta\varepsilon_{AB}^J}{c\tau} = \frac{\Delta\delta\Phi_{AB}^J - \Delta\delta\rho_{AB}^J}{c\tau} \tag{7}$$

TL has also developed its own software for the above frequency offset calculations. Corresponding broadcast ephemerides, observations from the two sites and coordinates of the remote site should be included to run the software. We can obtain the frequency stability and accuracy of a remote clock by performing (5) at the real-time processing and also performing (7) at the postprocessing. At the real-time processing, performance of a remote clock can be acquired as soon as possible. At the post-processing, its performance traceable to TL's frequency standard could be obtained.

IV. EXPERIMENTAL RESULTS

First, we compared 5 MHz output of a hydrogen maser with TL's standard frequency using a SR620 time-interval counter and the RFCS respectively. Measurement results of the SR620 are used here to evaluate the performance of the RFCS. The measurement time is 1 day with an observation interval of 30(s), so we totally have 2880 sampling data from each measurement instrument. The GPS receiver's antenna installed at the remote site is about several meters away from the one at the master site. In Figure

2, it is seen that not only the frequency stability, but also the time difference, from both instruments match each other quite well. This proves the feasibility of our RFCS and developed software.

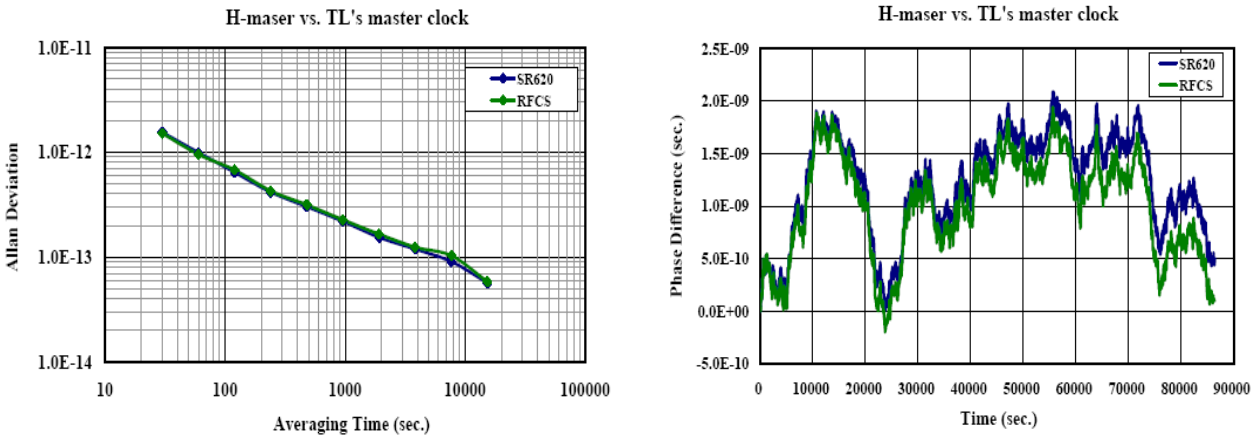

Figure 2. 5-MHz output of a hydrogen maser compared with TL's standard frequency using a SR620 and the RFCS respectively: (a) frequency stability comparison; (b) phase difference comparison.

Second, a common-clock short-baseline test was carried out to obtain performance limitation of the RFCS. Because we want to compare the results to frequency stability from specifications of a 5071A cesium clock, the measurement time was set to 1 week with observation interval 1 (s). TL's frequency standard was used as the common clock here. In Figure 3(a), we can see performance of the RFCS is better than that of a high-performance cesium clock when $\tau > 3$ (s) and a standard-performance one while $\tau > 2$ (s). Next, the remote site was moved to Kaohsiung, which is 270 km away from the master site at TL. A high-performance cesium clock and TL's frequency standard were frequency references used at the remote site and the master site separately. In this situation, performance of the RFCS degrades as shown in Figure 3(b). Its performance still excel that of a standard-performance cesium clock for $\tau > 2$ (s), but only excel that of a high-performance one for 4 (s) $< \tau <$ 200 (s).

In order to find out factors that influence performance of the RFCS in the 270-km baseline test, we used a dual-frequency GPS receiver to replace the original single-frequency one at the remote site, with the Bernese GPS software for data analysis. In Figure 4, results show that its performance could be improved to be a small amount better than that of a high-performance cesium clock while $\tau > 4$ (s).

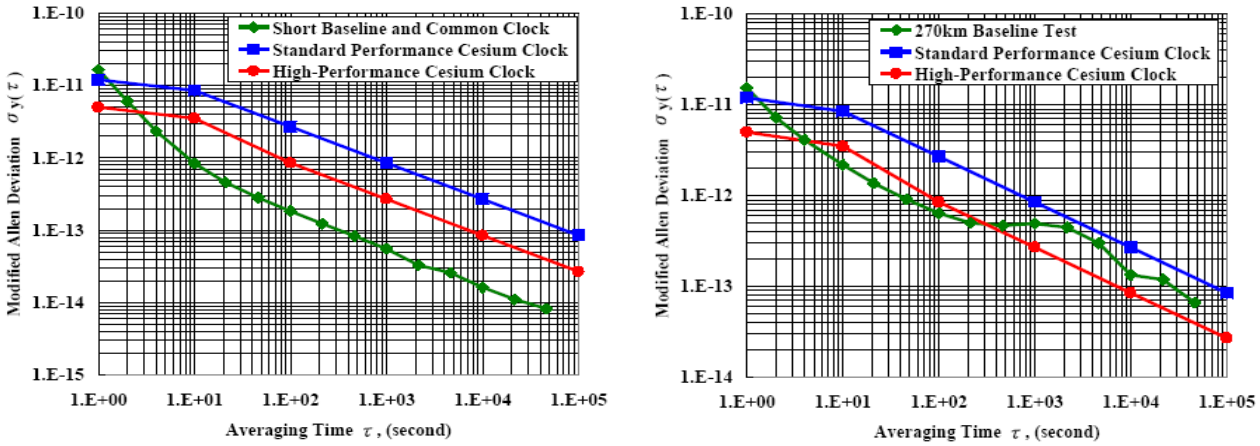

(a) (b)

Figure 3. (a) Common-clock short-baseline test results vs. frequency stability from specifications of a 5071A cesium clock; (b) 270-km baseline test results vs. frequency stability from specifications of a 5071A cesium clock.

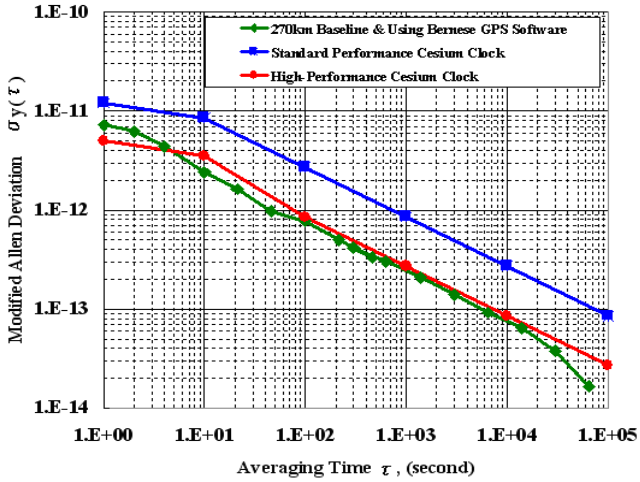

Figure 4. 270-km baseline test using a dual-frequency GPS receiver and Bernese GPS software.

V. CONCLUSIONS

In this paper, we introduce the remote frequency calibration system using GPS carrier-phase technique at TL. Customers can monitor real-time performance of their frequency sources with respect to the GPS time by the stand-alone system. If they need the sources traceable to TL's frequency standard and a higher measurement resolution, postprocessing conducted at the master site could meet their requirements.

We have carried out some tests to reveal performance of the RFCS. While in phase comparisons of a hydrogen maser vs. TL's frequency standard, the experimental results of our RFCS show good agreement

with those of a SR620 time-interval counter. This proves the feasibility of the RFCS and developed software. In the common-clock short-baseline test, frequency stability of the system could reach 2.0×10^{-11} per second and 8.0×10^{-15} per day, which also indicates its potential to measure a high-performance 5071A cesium clock for $\tau > 3$ (s) and a standard-performance one for $\tau > 2$ (s). If the baseline is extended to 270 km, the frequency stability of the system degrades and can't meet the requirements of a high-performance 5071A cesium clock. A dual-frequency GPS receiver was then substituted for the original single-frequency one at the remote site, with the Bernese GPS software for data analysis, and experimental results indicate that the system reclaims the potential to measure a high-performance 5071A cesium clock. This means if a single-frequency GPS receiver is used at the remote site for frequency calibration, detailed information about ionospheric and tropospheric delays should be considered to assure performance of the RFCS, which is very important especially in long-baseline measurement.

REFERENCES

[1] J. A. Davis and J. M. Furlong, 1997, "*Report on the study to determine the suitability of GPS disciplined oscillators as time and frequency standards traceable to the UK national time scale UTC(NPL),*" Centre for Time Metrology, National Physical Laboratory, UK.

[2] F. Cordara and V. Pettiti, 1999, "*Short term characterization of GPS disciplined oscillators and field trial for frequency of Italian calibration centers,*" in Proceedings of the 1999 Joint Meeting of the European Frequency and Time Forum (EFTF) and the IEEE International Frequency Control Symposium (FCS), 13-16 April 1999, Besançon, France (IEEE Publication 99CH36313), pp. 404-407.

[3] B. Hofmann-Wellenhof, H. Lichtenegger, and J. Collins, 1994, **Global Positioning System: Theory and Practice** (Springer-Verlag, Vienna).

[4] D. Wells, 1996, **Guide to GPS Positioning** (Canadian GPS Associates).

[5] S.-S. Chen, H.-M. Peng, and C.-S. Liao, 2001, "*Monitoring the remote primary clock by using GPS carrier phase,*" in Proceedings of the 33rd Annual Precise Time and Time Interval (PTTI) Systems and Applications Meeting, 27-29 November 2001, Long Beach, California, USA (U.S. Naval Observatory, Washington, D.C.), pp. 233-240.